Geodynamics of Iceland and the North Atlantic Area

edited by

L. KRISTJANSSON

NATO ADVANCED STUDY INSTITUTES SERIES

Series C: Mathematical and Physical Sciences

MARINE HEAT FLOW MEASUREMENTS IN THE NORWEGIAN-GREENLAND SEA AND IN THE VICINITY OF ICELAND

Marcus G. Langseth and Gary W. Zielinski

Lamont-Doherty Geological Observatory, Palisades, New York 10964 and Department of Geological Sciences, Columbia University, New York, New York 10027, U.S.A.

ABSTRACT. We report 55 new measurements of heat flow in the Norwegian-Greenland Sea and 29 new measurements on the flanks of the Reykjanes Ridge. Interpretations of the data are based only on the most reliable measurements in areas with a low probability of environment disturbance to the heat flow. The results in the Norwegian-Greenland Sea show the expected decrease in heat flow with distance from the presently active spreading center. Based on a simple thermal model of sea-floor spreading, the average heat flow in the Norwegian-Greenland Sea over areas of the sea floor that can be dated is 2.7 HFU, which is anomalously high compared to other oceans of comparable age. Measurements at distances greater than 100 km from the Reykjanes Ridge axis show a steady decrease with age, and when age is taken into account the heat flow is also anomalously high relative to other spreading centers.

1. INTRODUCTION

Iceland appears to lie within a broad oceanic region of relatively high heat flow. This result implies the occurrence of relatively high temperatures at shallower depths. To explain this phenomenon it is not necessary to assume that comparatively more heat is being brought to the base of the lithosphere in the vicinity of Iceland. The fundamental requirement is that the ratio of the heat being brought to the base of the lithosphere to that being dissipated via the sea-floor spreading mechanism be greater for this region than for other oceanic spreading centers.

Kristjansson (ed.), Geodynamics of Iceland and the North Atlantic Area. 277-295.

Much of the discussion of this conference has focused on the fact that the spreading center in Iceland is anomalous compared to most spreading centers in the world. Recently Iceland has come to be viewed as a "hot spot" and considerable significance has been placed on such hot spots as a key to processes in the mantle. Evidence is increasing that Iceland is but the emerged part of a much larger anomalous oceanic region. The ridge to the south of Iceland, the Reykjanes Ridge, is characterized by relatively shallow depth and positive free-air gravity anomalies. Similarly, abnormally shallow basin depths and positive free-air anomalies are found in the Norwegian-Greenland Sea to the north. If the shallow ocean floor in these regions is due to thermal expansion as a result of anomalously high temperatures in the lithosphere, this should be reflected in the heat flow at the surface.

In this paper we report a large number of new measurements made in the area during the past eight years principally from the R.V.VEMA and a few measurements made aboard the Russian research vessel, the AKADEMIK KURCHATOV (Tables 1 and 2). By comparison with heat-flow results in other oceans, we will show that the whole region north of the Charlie-Gibbs fracture zone at 53°N and the Norwegian-Greenland Sea has anomalously high heat flow. The direct implication of this result is that high temperatures exist at shallower depths below this region as compared with other oceanic spreading centers. These high temperatures could result from an imbalance between spreading rate in the area and heat flow from the mantle compared to spreading centers in more normal areas of the ocean.

The observations reported here were all made with the Ewing thermograd apparatus which is used on a piston corer [1]. By means of thermistor probes attached to the core barrel, temperature measurements at up to five depths in the sediment are made. The thermal conductivity of the sediment is determined by making measurements by the needle-probe method [2] on the sample returned in the corer. In Fig. 1 we show a typical record from the thermograd apparatus. After the corer penetrates the sediment, all of the traces corresponding to sediment probes are displaced upward, indicating higher temperatures. These temperatures when plotted versus depth show a linear increase (see Fig. 2) of about 1.0°C/10 m with depth. This gradient results from heat flow from depth. Fig. 2 also shows the results of conductivity measurements on the core sediments sample plotted versus depth. The gradient and conductivity determined over each interval are used to calculate the heat flow, which is shown in the right-hand plot. The heat flow calculated between the topmost and bottom-most point is shown as the dashed line.

TABLE 1

GEOTHERMAL DATA IN THE NORWEGIAN-GREENLAND SEA

Cruise	T'Grad Station #	Latitude	Longitude	Depth m	Grad. °C/l0m	Cond. Cal/°C cm sec	Heat Flow ucal/cm² sec.	Eval.	STATION ENVIRONMENT Topography		Sediment		Water
V-23	47	74°02'N	7°24'E	1928	1.90	2.35A*	4.47	8	rough ridge crest	VP**	thin covering	VP	NP
	49	77°57'	0°12'	3052	0.71	2.89	2.05	8	abyssal plain	NP	thick, flat lying	NP	NP
	51	76°59'	7°05'	2941	1.94	2.42A	4.69	8	side of mountain	VP	thin sediment pocket	VP	P
	53	72°04'	1°24'	2360	2.86	2.24A	6.41	9	axial mountain base	VP	small sediment pond	VP	NP
	54	70°59'	6°41'	3043	1.11	2.44A	2.74	8	abyssal plain	NP	thick, flat lying	NP	NP
	55	64°48'	1°19'W	2930	0.32	3.86	1.24	10	gently sloping basin	NP	thick, layered	NP	NP
	56	63°39'	1°22'E	1743	0.13	3.80	0.49	5	continental margin, flat	NP	thick sediment wedge	P	P
V-27	4	68°27'	13°32'W	1719	1.37	2.33	3.19	6	tilted sediment pocket	NP	.4 sec over sloping subbot.	NP	NP
	5	70°15'	13°05'	1392	1.08	2.13	2.30	6	irregular bottom	P	thin sediment pocket	P	NP
	7	74°28'	1°41'	3607	1.14	2.70	3.08	7	small, rolling hills	NP	thick, stratified	NP	NP
	9	73°04'	4°49'E	2297	N/L	2.39	-	7	axial mountains	VP	U-shaped sediment pocket.	VP	NP
	10	72°11'	8°35'	2537	0.85	2.34	2.00	7	abyssal plain	NP	thick, flat lying	NP	NP
	11	71°19'	12°04'	2299	0.60	2.58	1.54	6	abyssal plain	NP	thick, flat lying	NP	NP
	12	70°24'	14°47'	2429	0.78	2.48	1.94	5	gently sloping	NP	thick, slightly tilted	NP	NP
	21	78°24'	7°25'	2919	1.06	2.95	3.13	5	large V-shaped valley	VP	thick pocket	P	NP
	23	74°59'	10°50'W	2897	0.87	2.85	2.48	4	shelf edge	VP	thick, stratified	P	NP
V-28	16	68°47'	20°46'	1326	1.70	1.81	3.08	9	flat portion of trough	NP	thick, stratified	NP	NP
	18	70°48'	18°19'	1677	1.00	2.50	2.50	9	flat, continental margin	NP	thick, flat lying	NP	NP
	19	72°26'	13°39'	1283	0.54	3.19	1.72	7	flank of sharp ridge	VP	thin wedge	VP	P
	21	75°10'	10°52'	2462	0.61	2.53	1.54	8	hilly, continental slope	P	small pocket	P	NP
	22	76°49'	1°20'	3137	0.68	2.70	1.84	8	flat basin	NP	thick, slightly sloping	NP	NP
	28	62°54'	0°35'E	1171	0.21	3.00	0.62	5	continental slope	P	thick sediment wedge	NP	NP
	29	68°43'	12°43'W	1822	N/L	2.47	-	8	flat, large basement relief.	P	1/3 sec. sediment covering	NP	NP
	30	72°04'	9°04'	2398	0.88	2.35	2.07	8	rough bottom over irreg. subbot.	VP	thick but irregular.	VP	NP
	31	69°23'	4°24'	3449	1.11	2.26	2.51	8	base of mountain	VP	small wedge at base	P	NP
	32	67°53'	1°56'	3376	1.09	2.48	2.70	8	rough	VP	small sediment pocket	VP	NP
	37	74°00'	4°14'E	3148	0.81	2.28	1.85	5	very rough	VP	small sediment pocket	VP	NP
	38	70°56'	9°23'	2716	0.66	2.00	1.32	7	flat	NP	thick, flat lying	NP	NP

TABLE 1 (Continued)

Cruise	T'Grad Station #	Latitude	Longitude	Depth m	Grad. °C/10 m	Cond. Cal/°C cm sec	Heat Flow ucal/cm² sec	Eval.	STATION ENVIRONMENT Topography		Sediment		Water
V-29	138	66°44'	6°44'W	2459	0.71	2.41	1.71	8	gentle slope	NP	very thick	NP	NP
	139	67°48'	6°41'	2549	0.77	2.22	1.71	7	gentle slope	NP	very thick, stratified	NP	NP
	140	70°09'	7°20'	1443	0.81	2.27	1.84	9	broad, flat terrace	NP	thick, stratified	NP	NP
	142	72°58'	6°59'	2609	0.92	2.48	2.28	8	smooth, low relief peaks	NP	thick conformable	NP	NP
	143	75°56'	5°07'	3129	0.70	2.35	1.65	7	smooth, gentle slope	NP	thick stratified	NP	NP
	144	73°48'	0°06'E	2964	0.48	2.42	1.16	6	near scarp, undulating bottom	VP	rapidly thickening pocket	P	NP
	145	70°54'	4°55'W	1939	1.23	2.79	3.43	7	steep slope	VP	thin sediment pocket	VP	NP
	146	68°23'	5°26'	3411	0.93	2.18A	2.03	7	gentle slope	NP	thick, uniform	NP	NP
	147	65°11'	0°05'	2856	0.30	3.77	1.13	6	gentle slope	NP	thick, with unconformities.	NP	NP
V-30	98	67°31'	15°06'	860	1.81	2.03	3.68	9	flat plateau	NP	uniform 1/3 sec.	NP	P
	99	66°51'	9°02'	1595	0.90	2.02	1.82	9	flat	NP	thick, uniform	NP	NP
	100	65°05'	7°08'	2027	0.67	2.26A*	1.51	8	near scarp, rugged basement topo.	VP	thick V-shaped pocket.	NP	NP
	101	65°08'	5°18'	3812	0.81	2.26	1.84	9	flat floor of graben	NP	thick, stratified	NP	NP
	102	64°28'	4°57'	3316	0.71	2.26A*	1.61	8	narrow trough	P	pond	P	NP
	103	70°19'	9°32'	1308	1.08	1.82	1.97	10	steep peaks	VP	thin	P	P
	104	70°56'	16°56'	1472	1.26	2.14	2.70	10	low relief	NP	1/3 sec. draped sediments	NP	P
	105	71°29'	14°38'	1247	1.29	2.71	3.50	9	shallow broad ridge	NP	thick	NP	VP
	108	76°25'	2°15'E	3183	0.97	2.72	2.34	8	near steep peak	P	thick layer abutting peak	P	NP
	109	77°52'	4°08'	3075	0.89	2.67	2.36	7	smooth, floored, trough	NP	thick	NP	NP
	110	78°19'	2°00'	2006	0.63	3.10	1.94	7	top of broad ridge	VP	thick, stratified	NP	P
	111	76°17'	9°07'	2243	1.10	2.57	2.81	9	relatively flat	NP	thick, stratified	NP	P
	112	76°41'	6°52'	2413	>4.7	2.35	> 11	6	near rift valley edge	VP	thin	VP	NP
	113	70°11'	1°49'W	2905	0.96	2.67	2.57	8	gentle slope	NP	thick	NP	NP
	114	69°39'	2°30'E	3210	0.78	2.32	1.82	10	flat floored basin	NP	thick, stratified	NP	NP
	116	67°41'	8°24'	1918	0.75	2.76A	2.07	6	continental slope foot	P	thick, stratified	NP	P
	129	68°10'	5°45'	1911	0.52	2.70	1.40	10	gentle slope	NP	thick	NP	NP
	131	67°10'	6°05'	1236	0.38	2.58	0.98	10	fairly flat	NP	thick	NP	uncertain

* (A) indicates that the conductivity is assumed based on nearby values

** The letters NP, P or VP indicate our assessment of the probability of a significant disturbance to near surface heat flow by topography, sediment distribution and/or bottom water. NP = not probable; P = probable; and VP = very probable.

TABLE 2

NEW GEOTHERMAL DATA IN THE REYKJANES RIDGE AREA

Cruise	T'Grad Station #	Latitude	Longitude	Depth m	Grad. oC/10m	Cond. Cal/°C cm sec	Heat Flow ucal/cm² sec	Eval.	STATION ENVIRONMENT Topography		Sediment		Water
V-23	16	56°04'N	44°33'W	3259	0.73	2.03	1.48	10	flat near peak	P**	fairly thick	NP	NP
	19	59°46'	39°24'	2776	0.76	1.98	1.50	10	sloping	NP	thick	NP	P
V-28	9	60°25'	35°50'	3009	N/L	-	-	8	flat	NP	thick	NP	P
V-29	133	60°28'	20°58'	2603	1.27	1.73	2.19	7	gentle slope	NP	thick, undulating layers	NP	uncertain
	134	60°48'	22°26'	2087	1.17	1.87	2.20	10	rugged basement topography	P	fairly thick	NP	NP
	135	61°11'	23°50'	1851	1.26	1.80	2.28	10	irregular basement topography	NP	thick	NP	NP
	136	61°33'	25°08'	1441	0.54	1.79	0.96	10	atop plateau in rugged basement	NP	thick, stratified	NP	NP
	149	60°43'	26°38'	1699	0.86	1.91	1.64	10	large sediment pond	P	1/3 sec., fairly flat	NP	NP
	150	60°41'	27°15'	1304	2.83	1.98	5.60	8	top of flat topped Mount	P	1/4 sec. fairly flat	NP	NP
	151	60°41'	27°50'	1527	4.28	1.91	8.18	8	rugged	VP	small pocket	VP	NP
	152	59°22'	34°42'	3098	0.32	1.77	0.57	9	flat, broad basement depression	NP	thick	NP	VP
	153	57°50'	40°08'	3210	N/L	1.94	-	8	flat, irregular subbottom	NP	1/4 sec., stratified	NP	NP
	154	58°02'	42°48'	3208	0.98	2.04	2.02	8	flat	NP	fairly thick	NP	NP
	155	56°11'	44°42'	3300	0.82	2.01	1.65	9	flat corrugated	NP	thick	NP	NP
V-30	85	53°38'	44°16'	3686	0.81	2.02	1.65	10	hilly	NP	thick	NP	NP
	86	56°56'	44°53'	3504	0.79	2.03	1.61	10	flat	NP	1/3 sec., stratified	NP	NP
	88	56°50'	43°43'	3428	0.98	1.88	1.84	10	rolling	NP	thick, stratified	NP	P
	89	55°01'	43°53'	3392	0.83	1.92	1.54	10	low relief hills	NP	thick	NP	NP
	91	56°47'	38°34'	3306	0.88	2.28	2.01	10	broad topographical high	NP	thick	NP	NP
	93	57°52'	35°30'	2636	1.07	1.83	1.96	9	irregular	P	edge of sediment pocket	VP	NP
	94	58°34'	35°30'	2457	N/L	2.20	-	8	near sharp peak	VP	sediment pond	P	NP
	95	63°09'	35°32'	2542	0.82	2.22	1.83	10	gently sloping	NP	thick	NP	P
	96	64°04'	30°13'	2311	0.68	1.83	1.24	9	irregular	VP	thick, conformable	NP	NP
	132	54°03'	24°11'	3434	0.44	3.01	1.33	9	rolling	NP	thick	NP	NP

** The letters NP, P or VP indicate our assessment of the probability of a significant disturbance to near surface heat flow by topography, sediment distribution and/or bottom water. NP = not probable; P = probable; and VP = very probable.

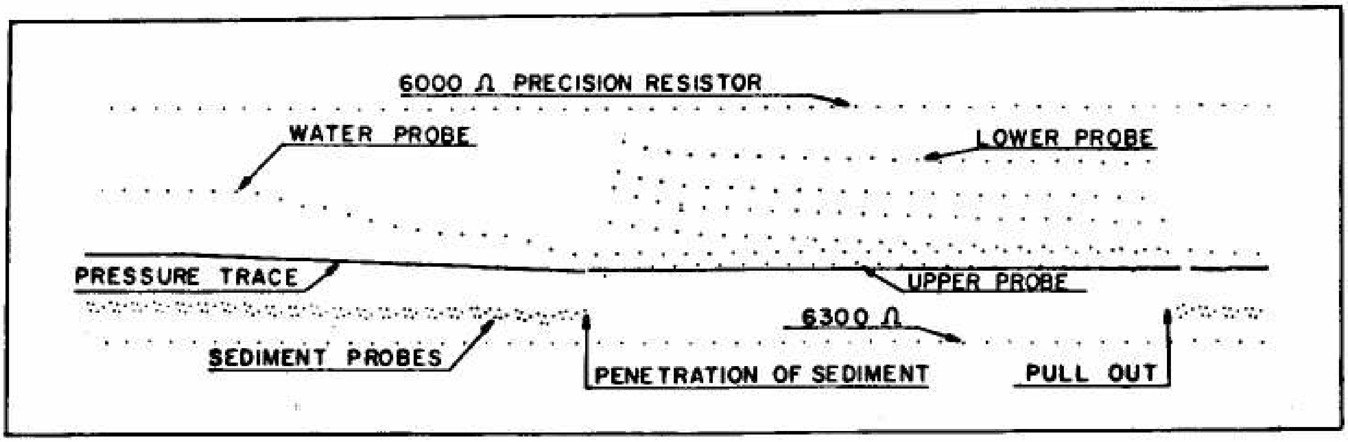

Fig. 1. A reproduction of a Ewing thermograd record showing the period during which the thermistor probes are in the sediment.

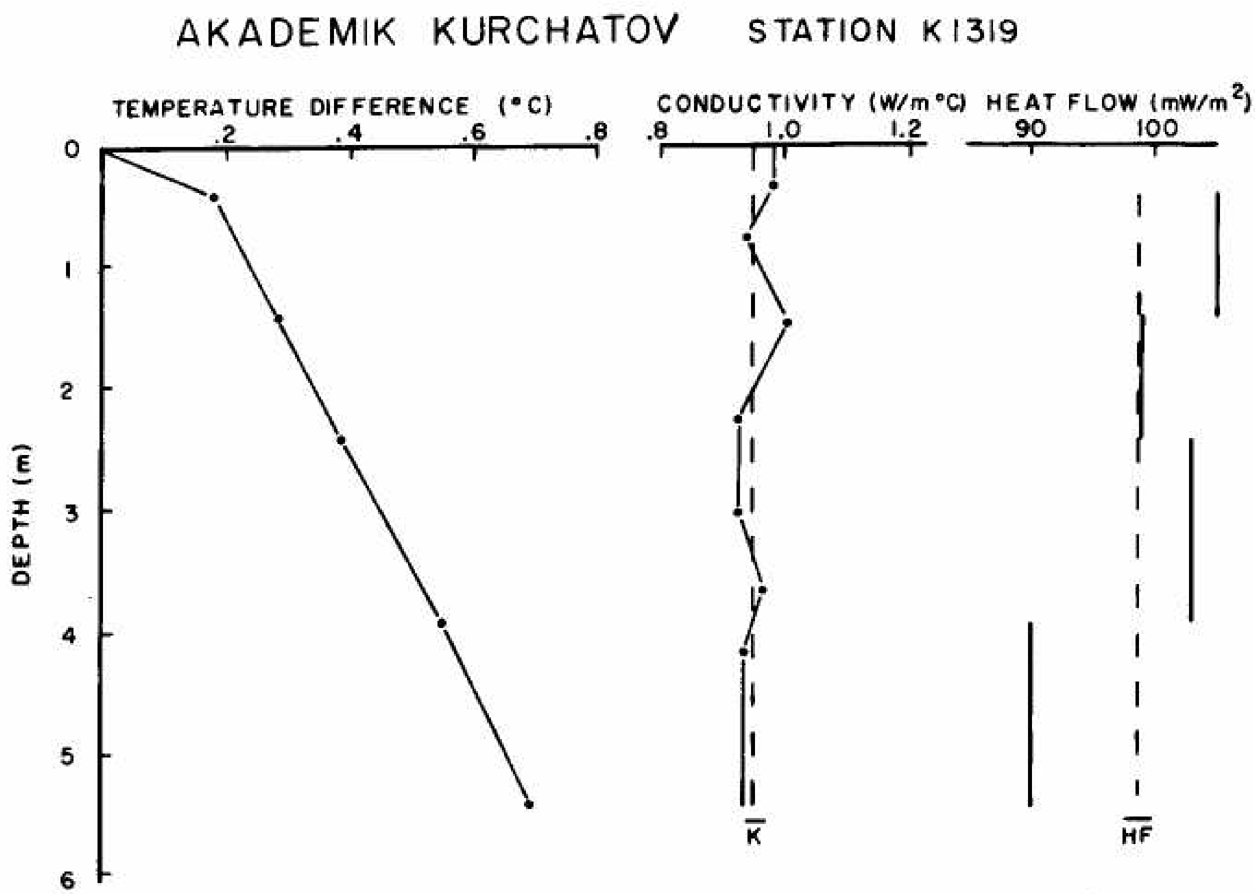

Fig. 2. Data from a thermograd station are shown plotted versus depth in the sediment. 41.8 mW/m^2 equals 1 $\mu cal/cm^2$-sec.

2. THE EVALUATION OF HEAT FLOW STATIONS

A most important part of the analysis is a critical evaluation of each heat-flow station. There are two parts to this evaluation: 1) an assessment of experimental procedure and instrument accuracy, and 2) an appraisal of the station's local environment and the probability of local disturbance to the near-surface heat flow.

The first part of the evaluation entails answering such questions as: How many probes penetrated the sediment and how deeply? Was the corer disturbed during the observational period? Was the recorder functioning properly? How accurate and representative are the conductivity measurements? Answers to these questions provide an evaluation of how reliable and accurate the heat-flow measurement at each station is. The evaluation for each station is given in Tables 1 and 2 and is based on a scale from 0-10. Generally, evaluations of 9-10 represent the most reliable and accurate stations; 7-8, good accuracy but reliability not firmly established; 4-6, stations of low accuracy and reliability; 0-3, unreliable measurements.

Regardless of how reliable a measurement is, it is equally important to know how representative it is of heat flow from the crust and mantle below the station. The "representativeness" of a station is assessed by examining the environment of each station to estimate the probability of local disturbance to the near-surface heat flow. In our evaluation we examine two major aspects of the environment: 1) the temperature stability of the bottom water, and 2) local topography and sediment distribution.

An appraisal of the temperature stability of the bottom water can be made from sediment and near-bottom water temperature measurements at the station. Measurements that show the heat flow is not uniform with depth in the sediment are probably made in areas of variable bottom water temperature. Large temperature gradients in the near-bottom water can make possible large excursions in bottom water temnerature and consequently transient disturbances to the near-surface heat flow.

It is well known that the surface heat flow is disturbed in areas of high-relief topography and patchy sediment distribution. See, for example, Von Herzen and Uyeda [3]. Seismic profiler records and echo-sounder records can be used to determine the proximity of a station to a large topographic feature or a sediment-rock boundary. Stations in close proximity to such features have a high probability of local disturbance.

Our evaluation of the probability of local disturbance to the measured heat flow is given in Tables 1 and 2 together with a brief description of the topographic and sedimentary environment. In the interpretation of the heat-flow results to be presented in the following sections, we have considered only data which have reliability and accuracy evaluations greater than 5 and a low probability of being locally disturbed. In general we find removing the unrepresentative and unreliable measurements greatly decreases the scatter of values. As a result regional averages and trends determined from the cleansed group of data should have greater significance.

3. RESULTS FROM THE NORWEGIAN-GREENLAND SEA

Since 1966 Lamont-Doherty Geological Observatory ships have made 55 successful measurements of heat flow in the floor of the Norwegian-Greenland Sea, which are shown on the map of Fig. 3. These stations are geographically well distributed over the area encompassed by the sea. At each of the stations the temperature and conductivity data have been carefully evaluated to determine the reliability of each heat-flow determination. The local topography, sediment distribution and bottom water temperature structure have been examined to assess the probability of local disturbance to the heat flow measured at each station. These assessments are presented in Table 1 together with the geothermal data.

Looking at the map of Fig. 3, we see that stations very near the axis of the Mohns and Knipovich Ridges yield very high values of heat flow. A heat flow greater than 11 HFU (1HFU $=10^{-6}$cal/cm^2 -sec) was observed at station V30-112. No measurements were made close to the Iceland-Jan Mayen Ridge axis; however, our measurements on the nearby flanks have relatively high values, i.e. 2.3-3.7 HFU. It is perhaps worth noting that, unlike other mid-ocean ridges, no station near the axis yielded very low heat flow although measurements at one station, V27-9, indicated heat flow that was not uniform with depth.

A line of heat-flow measurements on the western flank of the Iceland-Jan Mayen Ridge was reported by Lachenbruch and Marshall [4]. The locations of these stations are shown in Fig. 3. One of their stations, which is very near to our station V28-16, yielded a value of 2.67 HFU, whereas our station gave a value of 3.08 HFU. The principal difference was due to the gradient determination. Lachenbruch and Marshall gave strong evidence for appreciable variations in bottom water temperature in this area, and since their measurements were relatively shallow, <3 m, there is a possibility that the observed difference results from transient heat flow in the upper sediment induced by bottom water variations, particularly if the variations are aperiodic.

We have examined the heat-flow distribution relative to prominent morphological features and crustal age in three provinces separated by the two prominent fracture zones - the Jan Mayen fracture zone and the Greenland fracture zone. The values used in the following discussion are only the most reliable measurements that we have judged to have a low probability of local environmental disturbance. The distribution of values in the complex of basins,

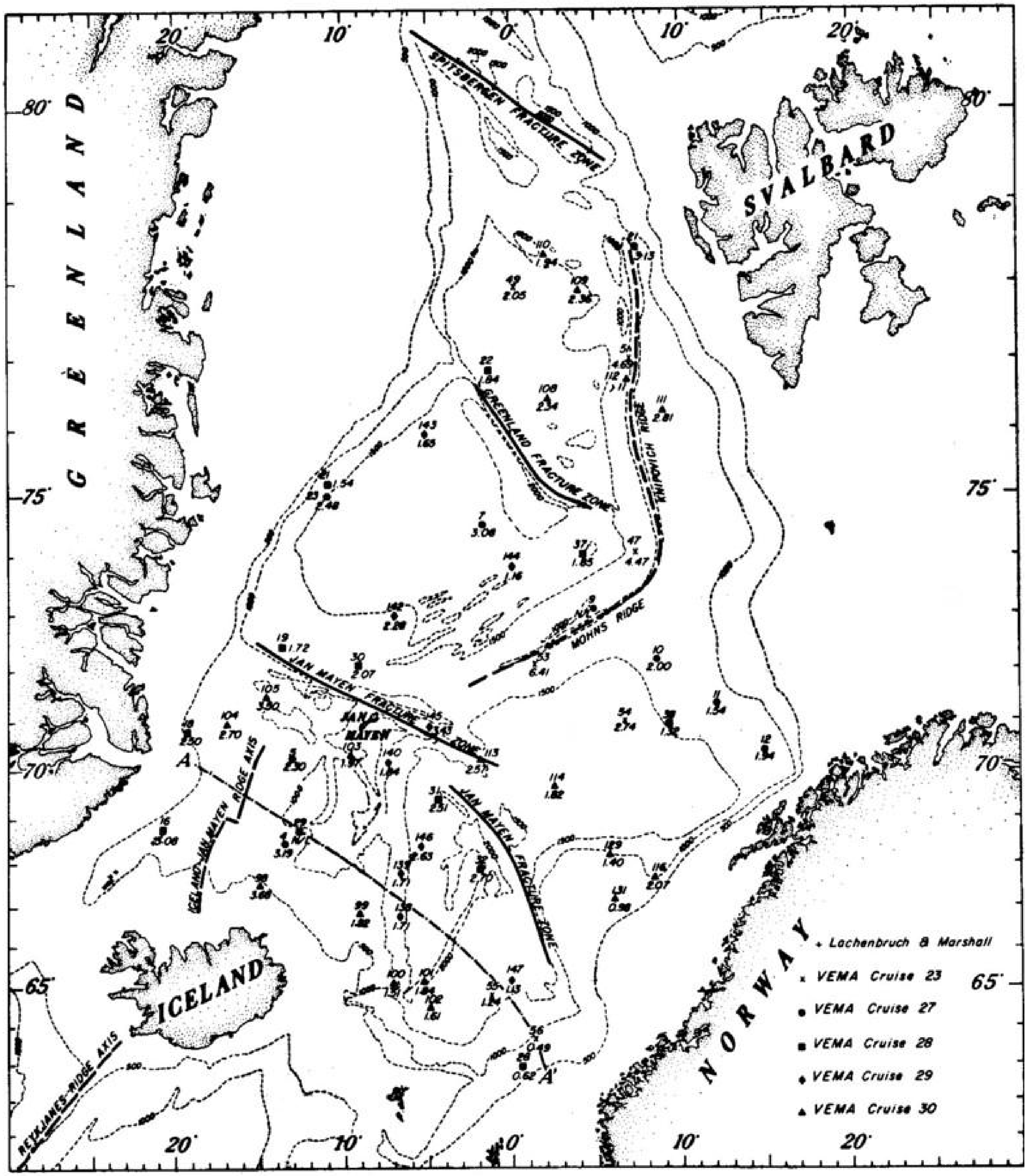

Fig. 3. Map showing the distribution of heat-flow stations in the Norwegian-Greenland Sea. The number above the symbol is the T'Grad station number. The number below the symbol is the heat-flow value for that station. N/L indicates a heat flow which is not uniform with respect to depth. The depth contours are in fathoms and are based on a map compiled by Talwani and Eldholm [7].

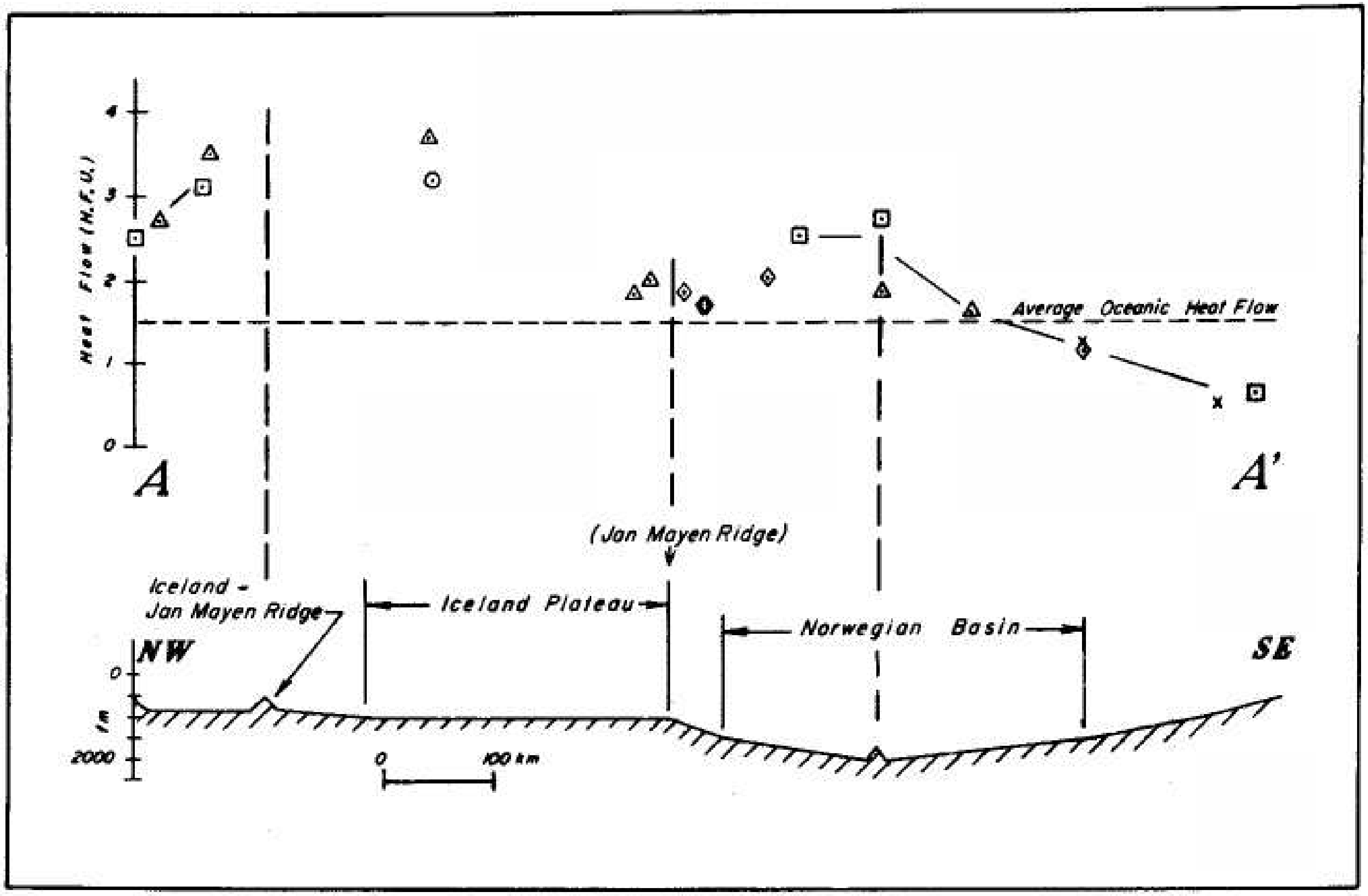

Fig. 4. Schematic section along A-A' in Fig. 3 across the Norwegian-Greenland Sea south of the Jan Mayen fracture zone showing the relation of heat flow to the various morphologic features in that area.

plateaus and ridges south of the Jan Mayen fracture zone are shown in profile by projecting the values on to Section A-A' in Fig. 3; the profile is shown in Fig. 4.

First we note a general decrease of heat flow from the northwest toward the southeast, reflecting the fact that the present active center of spreading lies near the western end of section A-A'. Four values on the western flank of the Iceland-Jan Mayen Ridge show a uniform decrease of heat flow from high values (3.5 HFU) to lower values (2.5 HFU) with increasing distance from the ridge axis.

Two values about twice the oceanic average (3.2-3.7 HFU) were measured over the eastern flank of the Iceland-Jan Mayen ridge complex. The values are relatively high considering their distance from the axis of the ridge. It is possible that these measurements are not associated with the present spreading center of the Iceland-Jan Mayen Ridge since they lie east of the well-defined magnetic pattern over this ridge [5].

A group of 5 measurements over the Jan Mayen Ridge and the region extending south from the ridge all indicate a heat flow of about 1.8 HFU. These values are relatively low compared to adjacent measurements and suggest that the Jan Mayen Ridge is thermally inactive relative to the Iceland-Jan Mayen Ridge and Iceland Plateau. In the Norwegian Basin relatively high values are observed over the area where Johnson and Heezen [6] have postulated a spreading center that became extinct at anomaly 7 time [7]. Values of 2.0-2.5 HFU would be expected over a ridge that became extinct 20-25 m.y.b.p. since, as we will show later, values in this range are found over crust of similar age in other parts of the Norwegian-Greenland Sea.

On the southeastern side of the Norwegian Basin there is a striking decrease of heat flow as the Norwegian continental margin is approached. Two values of 1.24 and 1.13 HFU were measured at the foot of the continental rise. These values are typical of older oceanic crust (>60 m.y.b.p.) in other areas of the world. The two easternmost values of 0.49 and 0.62 HFU are exceptionally low, but we believe these measurements are reliable. The two stations with very low values lie near the Faeroe-Shetland escarpment defined by Talwani and Eldholm [8]. The values are lower than the heat flow typically measured over the oldest oceanic and continental regions, 0.9-1.1 HFU; therefore, it is difficult to explain these very low heat flows in terms of a static crustal model. The conductivities measured at all four stations were abnormally high (3.0-4.0 mcal/cm-°C-sec). The sediments in the core samples contain a high percentage of sand and volcanic glass. Difficulties in conductivity measurement of sandy sediments are commonly encountered because of their tendency to lose water when opened. However, if we assume the conductivity measurements are unreliable and assume lower values typical of the western part of the Norwegian Basin, even lower heat flows would result.

Mohns Ridge appears to have been the most persistent spreading center during the evolution of the Norwegian-Greenland Sea Basin. Magnetic anomalies in the adjacent basins are well defined [7] so that we have plotted the heat flow on either side of Mohns Ridge against crustal age as shown in Fig. 5. On the same figure we show by solid dots the mean heat flow for various age provinces in the North Pacific reported by Sclater and Francheteau [9]. Comparison indicates that generally the heat flow over Mohns Ridge is greater than that of the North Pacific.

A similar plot is shown for data on the flanks of the Knipovich and Iceland-Jan Mayen Ridges (Fig. 6). A steady decrease of heat flow with age is seen and, as in the case of Mohns Ridge, these values all exceed the means of the North Pacific fcr regions of comparable age.

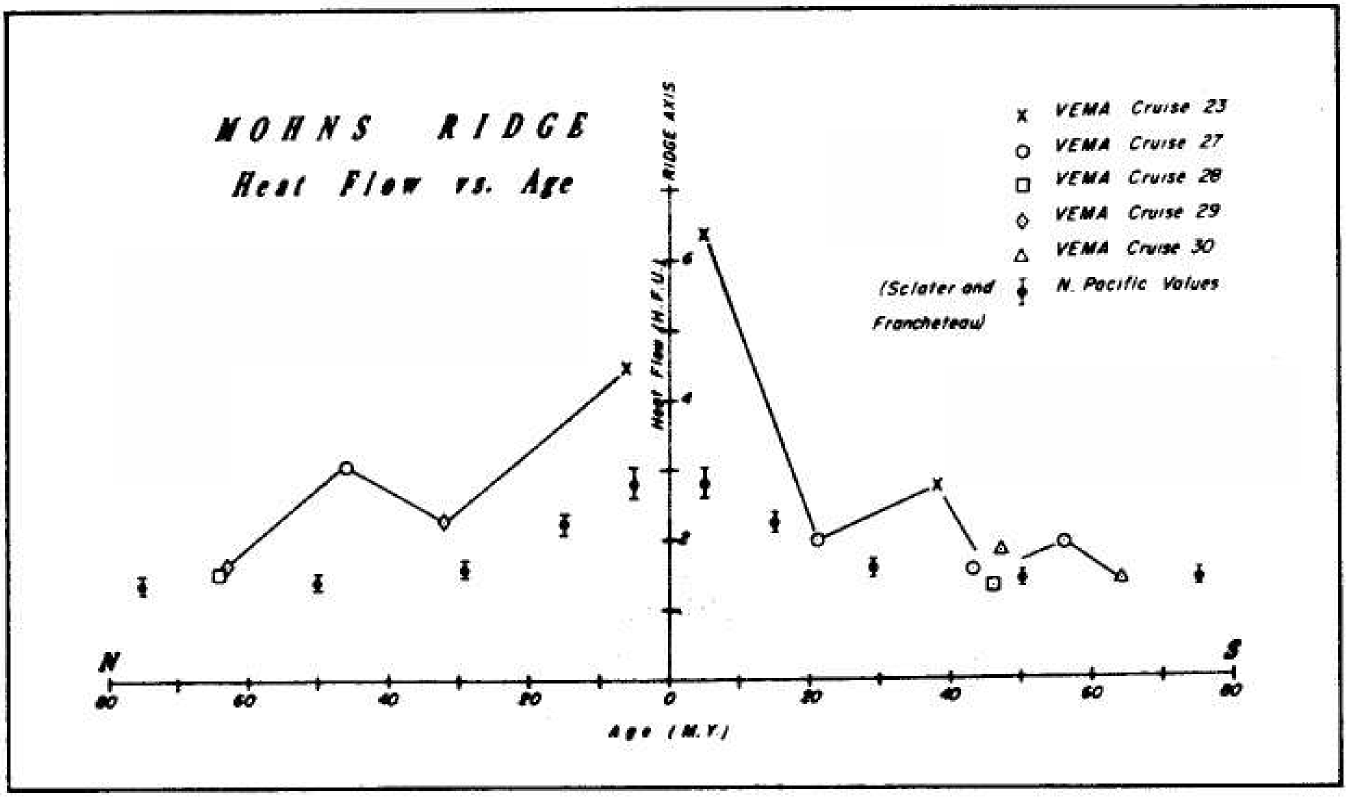

Fig. 5. Heat flow as a function of age of the oceanic crust for the Mohns Ridge area. The North Pacific average heat-flow values of Sclater and Francheteau [9] are plotted on both sides of the ordinate for comparison. The ages are based on the interpretations of Talwani and Eldholm [7].

4. A THERMAL MODEL OF THE LITHOSPHERE BELOW THE NORWEGIAN-GREENLAND SEA

All of the heat-flow measurements from the Norwegian-Greenland Sea where the magnetic anomalies permit an estimate of crustal age shown in Fig. 7. This combined data clearly show that heat flow in the Norwegian-Greenland Sea is higher than in the North Pacific for ocean crust of the same age. Over crust about 60 m.y. old, several stations in good agreement indicate heat flow is about 1.6 HFU.

We have attempted to fit the combined data of the Norwegian Sea, using the cooling plate model of McKenzie [10]. In this model the lithosphere is assumed to be a slab of uniform thermal properties moving away from the axis at a constant velocity. The accreting edge of the slab and the base of the slab are assumed to be an isotherm and the surface temperature is assumed to be a uniform colder temperature usually taken as zero. The lithosphere cools by conduction as it moves away from the axis.

To obtain a reasonable fit to the combined Norwegian-Green-

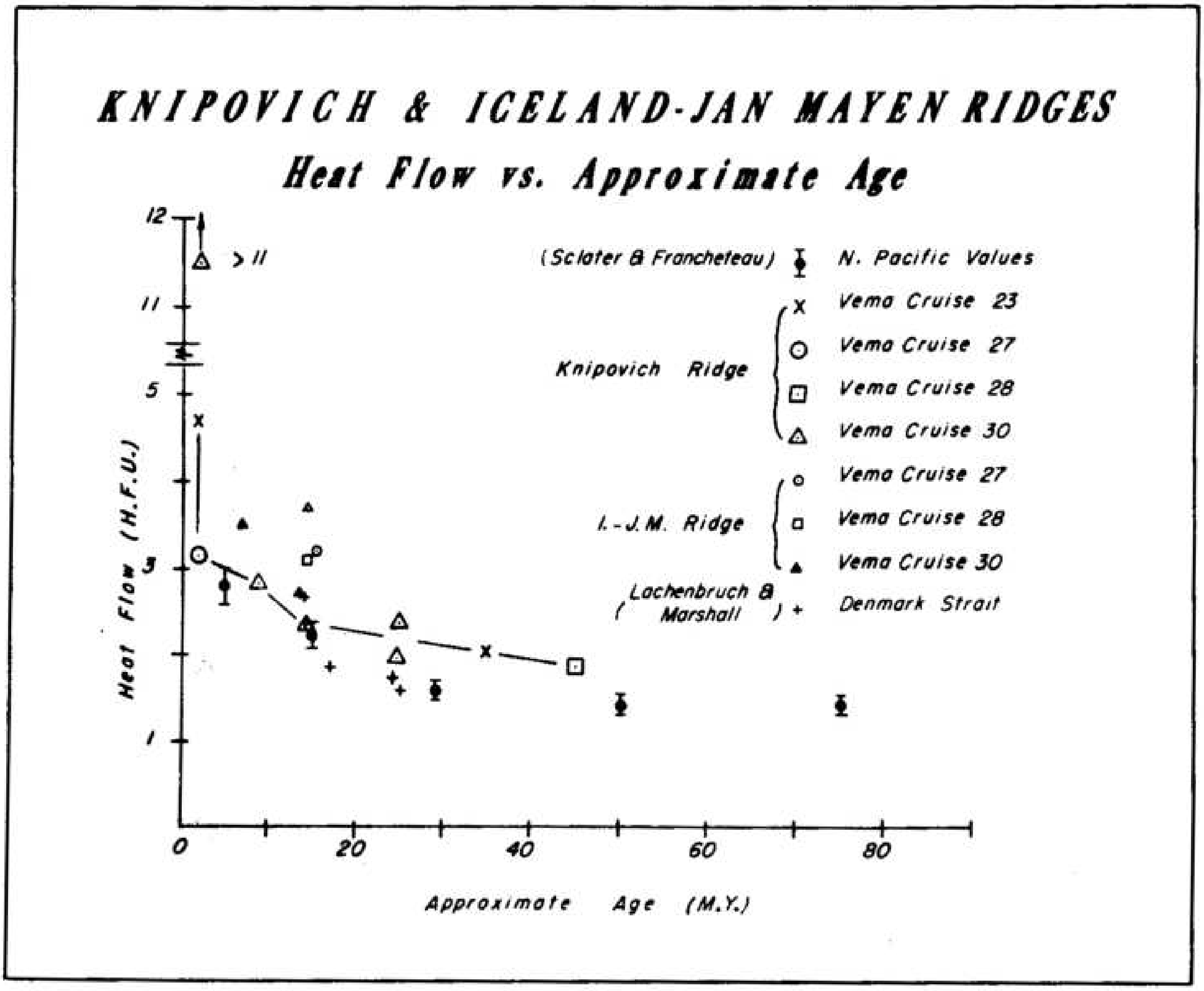

Fig. 6. Heat flow plotted as a function of approximate age of oceanic crust for the Knipovich and Iceland-Jan Mayen Ridge areas. The crustal age is based on the interpretation of magnetic anomalies by Talwani and Eldholm [7].

land Sea data we assumed a lithosphere 60 km thick with a temperature at the axis and base of the slab of 1475°C and a velocity of 1 cm/yr based on the magnetic lineations. The thermal conductivity of the lithosphere is assumed to be 0.007 cal/cm-°C-sec. The results of this model are shown by the solid line in Fig. 7. Such a fit is far from unique. An adequate fit could also be obtained with a basal temperature of 1250°C if the lithosphere were assumed to be 50 km thick rather than 60 km.

If we use the theoretical curve as a method to interpolate between the data and assume that heat flow within 10 km of the axis is 7.0 HFU, we find by integrating this curve that the average heat flow in the Norwegian-Greenland Sea is about 2.7 HFU - an average considerably higher than that over other oceanic areas of comparable age. It is well known that the elevation of the sea were made within 100 km of the axis [12]. The area of the survey is shown by the rectangle in Fig. 8. Since that survey was made we have had an opportunity to make 29 successful measurements over the broad region between Iceland and the Charlie-Gibbs fracture zone. Four of these stations over the axis of the ridge were made aboard the AKADEMIK KURCHATOV last summer. The geothermal data for these new stations except for the AKADEMIK KURCHATOV stations are given in Table 2. The locations of these stations and their heat-flow values are shown in Fig. 8. Most of the new observations lie on the western side of the ridge in the relatively shallow basin of the Irminger Sea between Greenland and the Reykjanes Ridge.

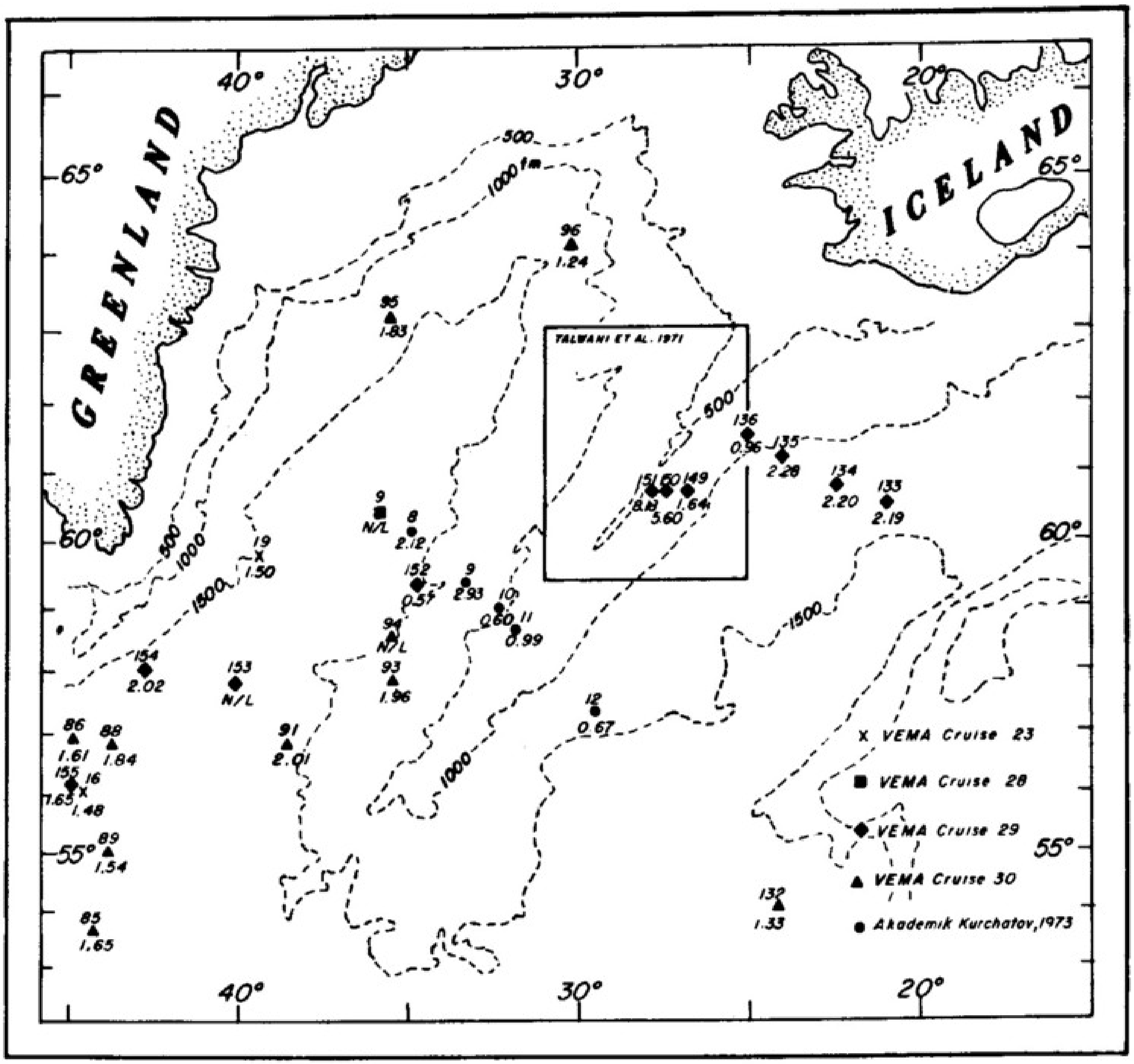

Fig. 8. Map showing the distribution of new heat-flow stations on the Reykjanes Ridge. The numbers above the symbols are T'Grad station numbers. The numbers below the symbols give heat-flow values. Depth is in fathoms. The rectangle outlines the area of an earlier comprehensive geophysical survey [12].

The earlier survey, during which numerous closely spaced observations were made, showed a rather complex pattern of heat flow relative to the ridge axis. One serious difficulty with observations over the shallower part of this ridge is the likelihood of variable bottom water temperatures. Temperature profiles in the sediment down to 10 m indicated that sea-floor heat flow in the shallower parts of the ridge (i.e. <1000 fm) was strongly affected by recent changes in the near-bottom water temperature. Consequently only gradient measurements deeper than 3-5 m would result mainly from heat flow coming from depth. Even after the effects of variable water temperature were eliminated to the extent possible, a confusing pattern of heat flow relative to the ridge axis resulted. In particular, a band of extraordinarily low values was observed at a distance of 70 km from the axis, and some stations within 30 km of the ridge axis yielded values from 1-2.3 HFU, which is near to or only slightly above the average of ocean basins.

Evidence is now strong that in regions near the axis of mid-ocean ridges where the sediment cover is relatively sparse, water circulation in the fractured upper crust may severely disturb the surficial heat flow [12,13]. If significant heat is being transferred by the convection of water, then the measurements of conductive heat flow in the sediment should underestimate the true heat flow. Substantial water circulation in the upper crust would also explain the large scatter of heat-flow values which has always characterized measurements in the axial zone.

We note that some of our new observations quite near the axis are below normal (three KURCHATOV stations and a VEMA 29 station). On the other hand, a line of three stations on the eastern side of the axis at about 60.5°N measures very high heat flows within a few tens of kms of the axis. In general, the values within 100 km should not be used to assess the heat flow from the Reykjanes Ridge until the thermal processes that transfer heat from depth to the sea floor are better understood. This is not true for measurements at greater distances from the axis. In these areas the sediment cover is generally thicker and more uniform which masks the thermal effects of water circulation in the crust beneath. The thicker sediment also diminishes possible effects of basement topography. Far from the axis, water depths are greater so that the probability of bottom water variations affecting the heat flow are minimized. The uniformity of values in these regions exemplified by the group of measurements south of Greenland and on the eastern flank of the ridge (see Fig. 8) further indicates the absence of large surficial disturbances in those areas.

When we examine the distribution of heat-flow values relative to the ridge axis, combining the new data with previous results,

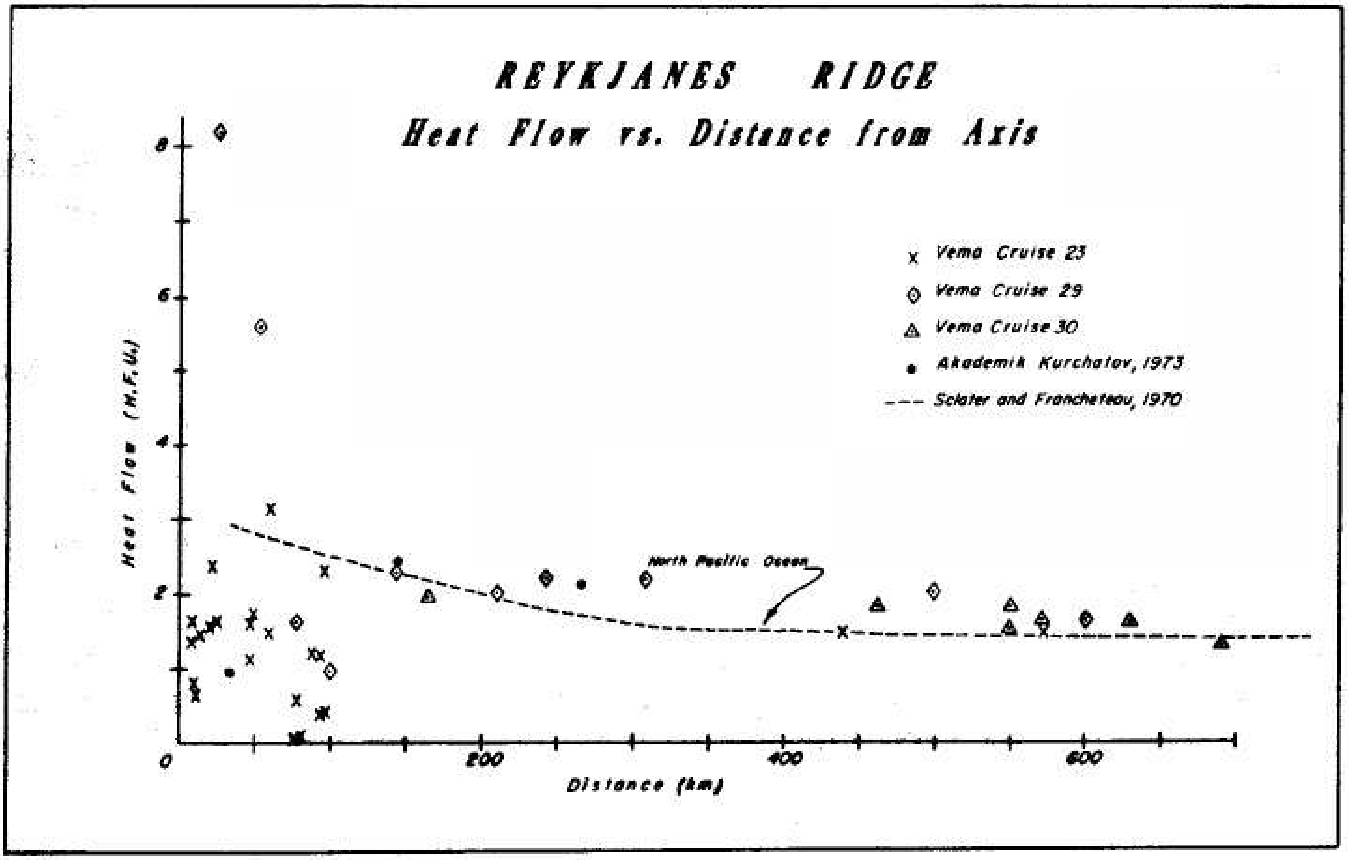

Fig. 9. Heat flow as a function of distance from the axis of the Reykjanes Ridge. The dashed line is the same as in Fig. 7.

we obtain a quite different conclusion than previously reported based on values close to the ridge axis. In Fig. 9 the values are plotted versus distance from the axis. The dashed line represents the North Pacific heat flow-versus-age data assuming a spreading rate of 1 cm/yr for the Reykjanes Ridge. The great scatter and predominantly low values within 100 km of the axis are very apparent, but it is clear that when data farther than 100 km from the axis are considered, the heat-flow values lie above the North Pacific curve. The relatively high heat flow in particular is supported by the very reliable and quite uniform values between 400 and 600 km. These values average about 1.6 HFU, which is significantly higher than the mean heat flow through the floor of the North Atlantic basins south of 43°N [14].

The result that anomalously high heat flow characterizes this region retlative to the North Atlantic supports the conclusion of Haigh [15] that high temperatures lie at relatively shallow depths below the basins adjacent to the Reykjanes Ridge compared to the more southern parts of the North Atlantic. Haigh's conclusions were based on thermal and petrochemical modelling of the gravity and topography of the area.

6. CONCLUSIONS

Our new results show that Iceland sits at the mid point of a vast region of anomalously high heat flow which extends from 53°N to as far north in the Norwegian Sea as we have measurements (∿80°N). The anomalous heat flow is accompanied by relatively shallow depths and positive free-air gravity anomalies. These observations are consistent with abnormally high temperatures at relatively shallow depth compared to other oceanic areas of the same age.

The sea-floor spreading mechanism is an efficient way for the mantle to lose heat. Heat is absorbed in the partial fusion of mantle material to make the basaltic crust. Large quantities of heat are brought upward near the surface by the formation of the crust and injection of material at the ridge axis, and once near the surface more effective cooling is possible by conduction. The general observation that heat flow and elevation of the ridges as a function of age over most oceanic spreading centers are very similar suggests that there is balance between spreading rate and heat flow from the deeper mantle to the base of the lithosphere, the faster spreading rates being associated with greater heat flow from the mantle.

One way of defining the anomalous conditions in the Iceland area is to state that the ratio of spreading rate to heat being brought to the base of the lithosphere is less there than is found over most spreading centers of the deep oceans. The main features of the oceanic region surrounding Iceland may result from the fact that the plates bounding the spreading center are not moving apart at a rate fast enough to dissipate heat flowing up from below to produce the lower heat flow, deeper ocean floor and thinner crust that we observe in most other so-called normal oceanic regions.

This point of view suggests that the cause of a hot spot of the Icelandic type may lie in the lithosphere's ability to respond to asthenospheric motions below it. If for some reason the plates bounding the region are prevented from rifting apart at a rate that forms a more normal ocean, then a hot spot will result. This would be a sufficient condition by this reasoning to form all the features we associate with Iceland and surrounding seas. It would not be necessary to call on heat coming up from the lower mantle, as is proposed in the mantle-plume hypothesis although such a mechanism is not ruled out.

The point we wish to emphasize is that the first-order diagnosis of the "Iceland hot spot" is a maladjustment between spreading rate and heat flow from the mantle compared to other oceanic spreading regimes. This diagnosis should be the starting point of conjecture about what "hot spots" tell us about the nature and mechanics of the asthenosphere beneath.

ACKNOWLEDGEMENTS

The data reported here were collected during a continuing geophysical survey of the Norwegian-Greenland Sea carried out over five summers during the past eight years. Much of the work was done as a cooperative program with the Norwegian Geotraverse Committee. The Lamont-Doherty Geological Observatory program has been led by M. Talwani, and we are grateful to him and O. Eldholm for use of their age interpretations before publication. We wish to acknowledge the indispensable help of Capt. H. C. Kohler, the scientific staff and crew of the VEMA. Annette Trefzer drafted the figures and Sivia Brodsky prepared the manuscript. G. Pálmason and G. Bryan read the manuscript and offered helpful criticisms. The data acquisition and research were supported by National Science Foundation grant GA27281 and Office of Naval Research contract N00014-67-A-0108-0004.

Lamont-Doherty Geological Observatory Contribution No. 2125.

REFERENCES

1. R. Gerard, M. G. Langseth Jr. and M. Ewing, J. Geophys. Res., 67, 785, 1962.
2. R. Von Herzen and A. E. Maxwell, J. Geophys. Res., 64, 1557, 1959.
3. R. Von Herzen and S. Uyeda, J. Geophys. Res., 68, 4219, 1963.
4. A. H. Lachenbruch and B. V. Marshall, J. Geophys. Res., 73, 5829, 1968.
5. P. R. Vogt and O. E. Avery, J. Geophys. Res., 79, 363, 1974.
6. G. L. Johnson and B. C. Heezen, Deep-Sea Res., 14, 755, 1967.
7. M. Talwani and O. Eldholm, in prep., 1974.
8. M. Talwani and O. Eldholm, Geol. Soc. Am. Bull., 83, 3575, 1972.
9. J. G. Sclater and J. Francheteau, Geophys. J. Astr. Soc., 20, 509, 1970.
10. D. P. McKenzie, J. Geophys. Res., 72, 6261, 1967.
11. X. LePichon and M. G. Langseth Jr., Tectonophysics, 8, 319, 1969.
12. M. Talwani, C. C. Windisch and M. G. Langseth Jr., J. Geophys. Res., 76, 473, 1971.
13. C. R. B. Lister, Geophys. J. R. Astr. Soc., 26, 515, 1972.
14. M. G. Langseth Jr., X. LePichon and M. Ewing, J. Geophys. Res., 71, 5321, 1966.
15. B. I. R. Haigh, Geophys. J. R. Astr. Soc., 33, 405, 1973.